Published in final edited form as:
Acta Biomater. 2014 May ; 10(5): 2096–2104. doi:10.1016/j.actbio.2013.12.024.

Novel, Silver Ion Releasing Nanofibrous Scaffolds Exhibit Excellent Antibacterial Efficacy without the Use of Silver Nanoparticles

Mahsa Mohiti-Asli[1], **Dr. Behnam Pourdeyhimi**[1], and **Dr. Elizabeth G. Loboa**[3,4,*]

[1]College of Textiles at North Carolina State University, Raleigh, NC 27695, USA

[2]College of Veterinary Medicine at North Carolina State University, Raleigh, NC 27695, USA

[3]Joint Department of Biomedical Engineering at University of North Carolina at Chapel Hill and North Carolina State University, Raleigh, NC 27695, USA

[4]Department of Materials Science & Engineering, North Carolina State University, Raleigh, NC 27695, USA

Introduction

Although minor skin wounds can heal naturally, immediate coverage using skin substitutes is necessary for treatment of extensive or irreversible damages caused to skin (1). An ideal skin substitute should protect the wound from microorganism contamination and further physical damage while also accelerating the healing process and minimizing scarring (2). Many xenograft (3), allograft (4,5), and autograft (6,7) skin substitutes have been investigated for wound healing. However, due to limited donor sites from which to acquire autografts, risk of infection, slow healing, and scar formation associated with these approaches, creation of tissue engineered skin substitutes has become an active area of investigation (8). Many advancements in tissue engineered skin substitutes have been achieved in the past three decades using natural or synthetic polymeric scaffolds (9,10). From these studies, it is now understood that the polymeric materials used should meet specific requirements related to hemostatic and anti-adhesion properties, air and moisture permeability, and appropriate absorption properties such that extraneous body fluid is extracted while the wound bed is kept moist to prevent dehydration (11). Nanofibers created from biodegradable, biocompatible polymers encompassing these properties are an excellent option for skin tissue engineering. Nanofibers are morphologically similar to the native extracellular matrix (ECM) of skin and have been shown to promote cell adhesion, migration and proliferation, leading to faster healing (12,13). As a result of the beneficial outcome achieved with the use of nanofibers for normal skin healing, they have been recently explored as carriers for antimicrobial agents to prevent infection at a wound site.

Silver is well known for its antimicrobial properties and is highly toxic to a wide range of microorganisms (14). It is an FDA-approved (15) broad-spectrum biocide that kills over 650 disease-causing bacteria, fungi, viruses, and mold (14). There is no life-threatening risk

*Corresponding author. Tel.: +1 919 539 3966; Fax: +1 919 513 4015. egloboa@ncsu.edu.

caused by inhalation, ingestion, or dermal application (16). If silver penetrates into the human body, it enters the systemic circulation as a protein complex, and can be eliminated by the liver and kidneys (16). Therefore it is not dangerous to humans when delivered in the proper chemical form and concentration (16). Although silver is relatively inert, its interaction with moisture coming from the surface of the skin and with fluids in the wound bed leads to the release of silver ions. Silver ions are highly reactive and bind to bacterial DNA and RNA, denaturing them resulting in bacterial growth inhibition (17).

The key to optimizing the use of silver as an antimicrobial agent is to maximize the production of silver ions that can be achieved by increasing the surface area of metallic silver. Silver in the form of nanoparticles has been incorporated in nanofibers by either *in situ* generation of nanoparticles within the polymer (18–20) or dispersion of prepared nanoparticles in the system (*ex situ* synthesis) (21,22). However, the very small size of nanoparticles allows them to penetrate into the stratum corneum of skin (23,24) or diffuse within the cellular plasma membrane and interfere with a variety of cellular mechanisms (22,25). For this reason, in recent years, the FDA and others (26–28) have recently expressed concern with antimicrobial approaches incorporating silver nanoparticles.

New methodologies and approaches to harness the excellent antimicrobial properties of silver ions, without the use of nanoparticles, therefore need to be actively explored. One way to deliver silver ions is to use silver nitrate with a suitable polymeric binder. In this study we investigated delivery of silver nitrate through a proprietary polymeric binder in a water/ethanol solution (Silvadur ET, Dow Chemical Company, Midland, MI, USA). We hypothesized that the polymeric binder would adhere to the surface of PLA nanofibers, provide an insoluble coating when water and ethanol were evaporated, and release silver ions capable of killing a variety of clinically relevant bacteria both in vitro and in vivo. We further hypothesized that an appropriate concentration of silver release could be achieved using this system to simultaneously kill and inhibit growth of bacteria but maintain viability and proliferation of human skin cells.

1. Materials and Methods

2.1. Nanofibrous Scaffold Fabrication

Polylactic acid (PLA), a biodegradable, biocompatible polymer with a molecular weight of 70000g/mol was dissolved in chloroform and dimethylformamide (both obtained from Sigma, St Louis, MO, USA) at a ratio of 3 to 1 to create a 12% solution. The mixture was stirred on a magnetic stirrer plate for at least 4 hours at 80°C until a homogeneous solution was obtained. Polymer solutions were used within 24 hours of preparation to eliminate evaporative loss of solvent and consequent change in solution concentration. The PLA solution was electrospun using 15 kV voltage, feed rate of 0.7 μl/hr and spinning distance of 13–15 cm. Silvadur ET solution at varying concentrations was used to coat the PLA nanofibers. Specifically, the initial concentration of silver in Silvadur ET is 1.0 mg/ml. This solution was diluted in deionized water to reduce the amount of silver within the solution to concentrations of 500, 250, 125, 62.5, 31.25, and 15.75 μg/ml. Nanofibers were dipped in the diluted Silvadur ET solution for one hour and then dried under a fume hood for 24 hours to form a thin antimicrobial coating. Coated nanofibers were then sterilized with ethylene oxide gas for 12 hours. Sterilized samples were rinsed with phosphate buffered saline (PBS) three times prior to each experiment.

2.2. Scaffold characterization

The thickness of the scaffolds was measured with a Mitutoyo absolute micrometer (Aurora, IL). Average thickness from at least 30 measurements was calculated. Field emission

scanning electron microscopy (FESEM JEOL 6400 F) was used to characterize surface morphology and microstructure of the ultra fine electrospun fibers at 15 kV and 200 kV accelerating voltage, respectively. Using SEM images, average fiber diameter of the scaffolds was calculated from at least 50 measurements per scaffold. To confirm the presence of the silver coating, X-ray photoelectron spectroscopy (XPS) was performed using a Kratos analytical axis ultra spectrometer (Chestnut Ridge, NY) for at least three different locations of both non-coated PLA scaffolds and Silvadur ET coated samples. Presence and uniformity of the silver coating was also verified by time-of-flight secondary ion mass spectroscopy (TOF-SIMS). TOF-SIMS analysis was performed on control PLA and Silvadur ET coated nanofibers using a TOF-SIMS V instrument (ION TOF, Inc. Chestnut Ridge, NY) equipped with a bismuth primary ion source (Binm+, n=1–5, m=1, 2). The chamber pressure was maintained below 5×10^{-7} Pa. The images were obtained for 500 μm×500 μm areas at 256×256 pixel resolution using Bi_3^+ primary ion beam.

2.3. Release profile of silver ions from PLA scaffolds

Scaffolds coated with Silvadur ET containing different concentrations of silver ranging from 15.75 to 125 μg/ml (release profiles of scaffolds containing 250 or 500 μg/ml silver were not analyzed as viability and proliferation analyses of human epidermal keratinocytes and human dermal fibroblasts (see Section 3.4 below) indicated these concentrations were toxic to human skin cells) were cut into 5×5 cm^2 squares, which weighed approximately 10 mg, and soaked in 5 ml deionized water and maintained in an incubator at 37°C and 5% CO_2 for two weeks. At the following time points: 24, 48, 84, 120 and 324 hours, the water was removed and replaced with fresh deionized water. The concentration of silver ions released in deionized water at each time point was quantified using a Perkin-Elmer AA300 atomic adsorption spectrophotometer (AAS) (PerkinElmer Inc. Waltham, MA).

2.4. Antimicrobial efficacy of scaffolds

Antimicrobial properties of the scaffolds were assessed against both gram negative (*Escherichia coli* J53) and gram positive (*Staphylococcus aureus*) bacteria as well as a silver (Ag) resistant bacteria (*E. coli* J53 [pMG101]) as a control to ensure that the antimicrobial properties of the scaffolds were a result of silver content alone. Cation-adjusted Mueller-Hinton (MH) broth and agar (Difco Laboratories, Detroit, MI, USA) were used to prepare bacterial cultivating medium. Isolated bacterial colonies were grown overnight in an incubator (37°C, 5% CO_2) from frozen samples on an agar plate. For Ag-resistant bacteria, 100 mg/ml ampicillin sodium salt (Fisher Scientific, USA) was also added to the agar plates. Antimicrobial activity of the scaffolds against different bacteria was determined by both a) qualitative evaluation, Antibacterial Activity Assessment of Textile Materials – AATCC 147 method, and using the b) quantitative evaluation with the Assessment Of Antimicrobial Finishes on Textile Materials - AATCC 100 method.

2.4.1. Qualitative analysis of antimicrobial efficacy: AATCC 147—For this analysis, also known as the “parallel streak method”, scaffolds were cut into circles (d=1.6 cm), placed on a lawn of bacteria in an MH agar plate, and incubated overnight at 37°C. Each lawn was prepared by spreading a 0.5 McFarland suspension of bacteria in phosphate buffered saline (PBS) using a sterile swab. The inoculants used included *S. aureus*, *E. coli* J53 and *E. coli* J53 [pMG101]. Bactericidal activity was visually assessed to determine the zone of inhibition around the fiber mat after overnight incubation per the AATCC 147 protocol to evaluate antimicrobial efficacy of the scaffolds against the inoculated bacterium.

2.4.2. Quantitative analysis of antimicrobial efficacy: AATCC 100—For quantitative evaluation, scaffolds were cut into 1cm^2 squares and soaked in 2 ml MH broth inoculated with *E. coli* or *S. aureus* bacteria at an initial concentration of 10^6 CFU/mL. To

control the accuracy of bacterial density, bacteria were diluted in PBS at 10^3, 10^4, 10^5, and 10^6 CFU/mL and plated overnight. Suspensions were then incubated at 37°C for one week. Bacterial concentration after incubation was determined via serial dilution of the suspension and spreading 100 μL of each diluent on a tissue culture plate. Evenly spread bacteria on plates allowed for isolation of individual colonies for quantification after overnight incubation. Non-treated PLA scaffolds were used as negative controls. Equation 1 (per AATCC 100 protocol) was used to calculate the reduction%:

$$Reduction\%=100(B-A)/B \quad (1)$$

where A is the number of bacteria recovered from the inoculated antimicrobial PLA scaffold after one week; and B is the number of bacteria recovered from the inoculated uncoated, control PLA scaffold. 0% reduction indicates no antimicrobial efficacy; 100% reduction indicates complete antimicrobial efficacy.

2.5. Biocompatibility assessment of scaffolds

Biocompatibility assessment of antimicrobial scaffolds was performed using human dermal fibroblasts and human epidermal keratinocytes derived from adult skin (2^{nd} passage, Lonza (USA)). Nanofibers coated with Silvadur ET containing different concentrations of silver: 250, 125, 62.5, 31.25 or 15.75 μg/ml, were cut into circles (d=1.6 cm). Sterilized samples were soaked in fibroblast or keratinocyte growth medium (Lonza, USA), respective to cell type being evaluated, for 24 hr and then seeded with cells at an initial density of 4×10^4 cells per scaffold. Cell-seeded scaffolds were then maintained in 1ml growth medium for 7 days at 37°C and 5% CO_2. Culture medium was replaced every three days.

2.5.1. Human skin cell viability—Cell viability was determined on days 1, 4 and 7 using a Live-Dead Assay Cytotoxicity Kit for mammalian cells (Molecular Probes, Eugene, OR). Specifically, cell seeded scaffolds were put in growth medium with the addition of 4 mM calceinacetoxymethyl ester-AM (staining the cytoplasm of live cells green) and 4 mM ethidiumhomodimer (staining the nuclei of dead cells red). The samples were then incubated for 20 minutes while protected from light.

2.5.2. Human skin cell proliferation—Cell proliferation was determined using the alamarBlue cell viability assay (AbDSerotec, Raleigh, NC) at days 1, 4 and 7 post seeding of cells on scaffolds. AlamarBlue, at a volume of 10% of the culture medium, was added to each well 7 hours before each measurement. After incubation with alamarBlue, 200 μL of each sample was taken in triplicate and the absorbency read at 600 nm using a microplate reader (TecanGENios, Tecan, Switzerland). AlamarBlue reduction% was then calculated from the absorbency results. A greater alamarBlue reduction% indicates greater cell proliferation.

2.5.3. Human skin cell morphology—Scanning Electron Microscopy (SEM) was used to visualize fibroblast and keratinocyte morphologies on the scaffolds. After 7 days of culture in growth medium, samples were fixed in 10% buffered formalin for 30 min and then dehydrated with a graded concentration (50–100% v/v) of ethanol. Dehydrated scaffolds were immersed in hexamethyldisilazane for 15 min and dried overnight under a fume hood. Dried samples were then sputter coated with gold to observe the morphology of cells using SEM.

2.6. Statistical analyses

Statistical analyses were performed using SPSS 14.0. The data was analyzed using a Duncan test with p-values less than 0.05 considered statistically significant.

2. Results and Discussion

3.1. Scaffold characterization

SEM images showed uniform nanofibers coated with Silvadur ET with an average fiber diameter of 460.53 ± 180 nm (Figure 1). There was no sign of formation of silver nanoparticles on the surface of nanofibers. The average thickness of the nanofibrous webs was 30±7 μm. XPS verified the presence of silver along the entire surface of nanofibers coated with Silvadur ET (Figure 2). In addition to silver, oxygen and nitrogen associated with nitrate (in silver nitrate: $AgNO_3$) were also uniformly distributed along the surface of all nanofibers. Presence of a carbon group as shown in the XPS analysis is a component of the polymeric binder in the Silvadur ET coating.

The presence of silver on the surface of Silvadur ET coated nanofibers was also verified by TOF- SIMS analyses. TOF-SIMS positive ion spectrum for pure PLA nanofibers only showed ions related to PLA including $C_3H_3O^+$, $C_3H_4O^+$, and $C_5H_7O_2^+$ (Figure 3). These ions were also detected in the spectrum for Silvadur ET coated PLA nanofibers but their intensity was lower, indicating the coverage of silver coating on the PLA nanofibers (Figure 3). Silvadur ET coated samples included different fragment ions of silver in the spectrum. Ions of $C_3H_5N_2^+$, $C_5H_7N_2^+$ in the coated PLA spectrum were associated with the binding polymer (Figure 3). In addition to confirming the presence of the silver coating on the surface of fibers, TOF-SIMS images also (Figure 4) allowed for mapping of the elements on the surface as a further indicator of coating uniformity. As seen in those images the Silvadur ET coating, comprised of the binding polymer and silver, were uniformly distributed along the fibers.

3.2. Release profile of silver ions from PLA scaffolds

One of the most important attributes of silver based antimicrobial bandages is the profile of silver release over time. For infected wounds, a rapid silver release upon bandage application is needed to clear the wound of contaminating microorganisms. A subsequent steady and prolonged release of silver at a minimum concentration level of 0.1 part per billion (ppb) can provide effective antimicrobial activity (29). In this work, release profiles of silver ions from antimicrobial scaffolds coated with different concentrations of silver within the Silvadur ET coating solution were determined. Results indicated a fast initial release of silver ions, followed by a gradual release of silver over two weeks, meeting the need for antimicrobial bandages (Figure 5). As expected, the amount of silver release was directly influenced by the initial amount of silver doped within the scaffolds. After two weeks the highest release (34.3 μg/ml) occurred with nanofibers coated with Silvadur ET containing the highest silver concentration evaluated, 125μg/ml, and the lowest release (9.8 μg/ml) was observed with scaffolds coated with Silvadur ET containing the lowest silver concentration, 15.75 μg/ml. This range of silver ion release is comparable with the release rate of silver from polyacrylonitrile nanofibers containing silver nanoparticles measured in similar conditions (release medium: deionized water, release temperature 37°C, ratio of sample weight to volume of the release medium: 2mg/ml) (30).

3.3. Antimicrobial efficacy of scaffolds

Qualitative analyses (AATCC 147) of the antimicrobial properties of the custom scaffolds against *E. coli* and *S. aureus* bacteria indicated clear zones of inhibition around all scaffolds with Silvadur ET coating (Figure 6). No zone of inhibition was observed against silver resistant bacteria indicating that the antimicrobial properties of the scaffolds were specifically a result of silver ion release. The zone of inhibition was measured for all scaffolds treated with Silvadur ET containing different concentrations of silver. There was

no significant difference between the zones of inhibition for scaffolds coated with different concentrations of Silvadur ET (Figure 7).

Quantitative antimicrobial analyses (AATCC 100) were performed for one week on scaffolds coated with different concentrations of Silvadur ET. Results indicated 100% reduction for all scaffolds in the presence of both *E. coli* and *S. aureus* bacteria. In addition to quantification via the AATCC 100 protocol, antimicrobial efficacy was also confirmed visually (Figure 8).

3.4. Biocompatibility assessment of scaffolds

There is always a concern about potential cytotoxicity to host mammalian cells associated with silver in wound dressings. Localized argyria, resulting in blue-gray pigmentation of skin, may result when silver compounds are applied directly on the skin. Although the National Institute for Occupational Safety and Health has set the daily exposure limit at 0.01 mg/m for all forms of silver to prevent argyria, it has been suggested that separate permissible exposure limits should be established for individual compounds (31). It has been shown that the cytotoxic effect of silver depends on dose, exposure time, and the cell line tested (32). Therefore, we evaluated the cytotoxic effects of our antimicrobial dressings containing different concentrations of silver, for up to 14 days, against the two primary cell lines in human skin: human dermal fibroblasts and human epidermal keratinocytes.

3.4.1. Viability of human dermal fibroblasts on scaffolds—Viability of human dermal fibroblasts grown on the antimicrobial scaffolds was assessed on days 1, 4 and 7. Results indicated that cells exhibited limited or no viability on scaffolds coated with Silvadur ET at concentrations of 125 μg/ml to 250 μg/ml silver in Silvadur ET coating solution (data not shown). However, the majority of cells remained viable on nanofibers coated with more dilute Silvadur ET concentrations containing 62.5 μg/ml and 31.25 μg/ml silver (Figure 9). Cells adhered to both coated and non-coated scaffolds and, in both cases, better adhesion of cells was achieved with extended culture duration (Figure 9).

3.4.2. Viability of human epidermal keratinocytes on scaffolds—Human epidermal keratinocyte viability was tested only on scaffolds that supported fibroblast viability (silver concentrations in coating solution: 62.5 μg/ml and 31.25 μg/ml) along with an additional scaffold coated with a lower concentration of silver, 15.75 μg/ml, in Silvadur ET solution. Human epidermal keratinocytes remained viable on all three of these scaffolds. Representative images of human epidermal keratinocytes on scaffolds with 31.25 μg/ml silver in the coating solution are shown in Figure 10 and were consistent for concentrations of 15.75 μg/ml and 62.5 μg/ml.

3.4.3. Proliferation of fibroblasts on antimicrobial scaffolds—Human dermal fibroblast proliferation was diminished on PLA scaffolds coated with higher concentrations of Silvadur ET (Figure 11). The reduction%, an indicator of cell proliferation, was almost constant over 7 days for scaffolds coated with the most concentrated Silvadur ET solution (250 and 125 μg/ml silver), indicating no cell proliferation on these scaffolds. These results support the findings from the viability analyses which indicated no viable cells on scaffolds with these silver concentrations. However, there was no significant difference in cell proliferation on scaffolds coated with the less concentrated Silvadur ET solution (31.25 μg/ml) relative to uncoated pure PLA scaffold controls at any time point (Figure 11).

3.4.4. Proliferation of human epidermal keratinocytes on the scaffolds—Proliferation of keratinocytes on the antimicrobial scaffolds followed the same trend as

fibroblasts and was decreased by an increase in silver concentration within the coating solution (Figure 12).

3.4.5 Morphology of cells on the scaffolds—SEM micrographs indicated that fibroblasts adhered and spread on the scaffolds (Figure 13). Fibroblasts spread throughout the surface of non-coated PLA nanofibers as well as fibers coated with Silvadur ET containing 31.25 and 62.5 μg/ml silver. However, for nanofibrous scaffolds coated with Silvadur ET containing 125 and 250 μg/ml silver, cells exhibited a rounded morphology, indicative of dead cells. These observations were consistent with the viability findings (Figure 9).

SEM analyses of human epidermal keratinocytes on antimicrobial scaffolds with Silvadur ET solutions containing 15.75 μg/ml, 31.25 μg/ml, and 62.5 μg/ml silver indicated cells adhered and spread on the scaffolds (Figure 14).

4. Conclusions

Silver ion releasing PLA nanofibrous scaffolds were developed using a silver ion releasing solution (Silvadur ET) comprised of silver nitrate, a proprietary polymer binder, water and ethanol. Multiple silver concentrations were created and evaluated as a coating solution on PLA nanofibers for antimicrobial efficacy. Nanofibers coated with solutions having different concentrations of silver ranging from 31.25 to 250 μg/ml exhibited excellent antimicrobial properties toward both gram positive and gram negative bacteria while having no effect on silver resistant bacteria. This verification against silver resistant bacteria was performed to confirm that the antimicrobial properties of these scaffolds was a result of silver content alone. Biocompatibility analyses of the antimicrobial scaffolds indicated that nanofibrous scaffolds coated with Silvadur ET solution containing silver equal to or less than 62.5 μg/ml maintained viability and proliferation of both human dermal fibroblasts and human epidermal keratinocytes. This is the first study to use a polymeric coating containing silver nitrate on nanofibrous scaffolds. These novel antimicrobial scaffolds are the first nanofibrous substrates that contain silver in a form other than nanoparticles to effectively address concerns related to the use of silver nanoparticles while still exhibiting excellent antimicrobial efficacy. Our findings indicate that silver can be used in nanofibrous bandages for wound healing applications if delivered in the appropriate form and concentration. We believe the clear-cut process for development of these antimicrobial scaffolds allows for facile utilization of these scaffolds/transdermal bandages with multiple applications in wound healing to allow for skin regeneration while maintaining antimicrobial efficacy.

Acknowledgments

This research was supported by NIH/NIBIB 1R03EB008790 (EGL), NSF/CBET 1133427 (EGL), Nonwovens Cooperative Research Center (Project 10-128, EGL), and the Chancellor's Innovation Fund (EGL). The authors would like to acknowledge Dr. Susan Bernacki for helpful discussions and all other members of the Cell Mechanics Laboratory.

References

1. Ruszczak Z, Schwartz RA. Modern Aspects of Wound Healing: An Update. 2000; 26:219–229.
2. Leung V, Hartwell R, Yang H, Ghahary A, Ko F. Bioactive nanofibres for wound healing applications. 2011; 4:1–14.
3. Chiu T, Burd A. "Xenograft" dressing in the treatment of burns. Clin Dermatol. 2005; 23:419–423. [PubMed: 16023938]
4. Leon-Villapalos J, Eldardiri M, Dziewulski P. The use of human deceased donor skin allograft in burn care. Cell Tissue Banking. 2010; 11:99–104. [PubMed: 20077178]

5. Wainwright DJ. Use of an acellular allograft dermal matrix (AlloDerm) in the management of full-thickness burns. 1995; 21:243–248.
6. Schwanholt C, Greenhalgh DG, Warden GD. A comparison of full-thickness versus split-thickness autografts for the coverage of deep palm burns in the very young pediatric patient. 1993; 14:29–33.
7. Branski LK, Mittermayr R, Herndon DN, Norbury WB, Masters OE, Hofmann M, Traber DL, et al. A porcine model of full-thickness burn, excision and skin autografting. Burns. 2008; 34:1119–1127. [PubMed: 18617332]
8. Zhong SP, Zhang YZ, Lim CT. Tissue scaffolds for skin wound healing and dermal reconstruction. 2010; 2:510–525.
9. Jones I, Currie L, Martin R. A guide to biological skin substitutes. Br J Plast Surg. 2002; 55:185–193. [PubMed: 12041969]
10. JTS, AG, SG. Skin substitutes and alternatives: a review. D - 100911021 2007. :493–508. quiz 509–10.
11. Boateng JS, Matthews KH, Stevens HNE, Eccleston GM. Wound healing dressings and drug delivery systems: A review. 2008; 97:2892–2923.
12. Charernsriwilaiwat N, Opanasopit P, Rojanarata T, Ngawhirunpat T. Lysozyme-loaded, electrospun chitosan-based nanofiber mats for wound healing. Int J Pharm. 2012; 427:379–384. [PubMed: 22353400]
13. Leung V, Hartwell R, Yang H, Ghahary A, Ko F. Bioactive Nanofibres for Wound Healing Applications. 2011:4.
14. Hong-bo W, Jin-yan W, Qiang W. Bacteriostasis of nanosized colloidal silver on nonwovens. 2006; 27:34–36.
15. Xing Y, Yang X, Dai J. Antimicrobial finishing of cotton textile based on water glass by sol-gel method. 2007; 43:187–192.
16. Lansdown A. Silver in health care: antimicrobial effects and safety in use. 2006; 33:17–34.
17. Rai M, Yadav A, Gade A. Silver nanoparticles as a new generation of antimicrobials. Biotechnol Adv. 2009; 27:76–83. [PubMed: 18854209]
18. Wang Y, Yang Q, Shan G, Wang C, Du J, Wang S, Li Y, et al. Preparation of silver nanoparticles dispersed in polyacrylonitrile nanofiber film spun by electrospinning. Mater Lett. 2005; 59:3046–3049.
19. Son WK, Youk JH, Park WH. Antimicrobial cellulose acetate nanofibers containing silver nanoparticles. Carbohydr Polym. 2006; 65:430–434.
20. Wang, Yongzhi; Li, Yaoxian; Yang, Songtao; Zhang, Guangliang; An, Dongmin; Wang, Ce; Yang, Qingbiao; Chen, Xuesi; Jing, Xiabin; Wei, Yen. A convenient route to polyvinyl pyrrolidone/silver nanocomposite by electrospinning. Nanotechnology. 2006; 17:3304.
21. Nimrodh Ananth A, Umapathy S, Sophia J, Mathavan T, Mangalaraj D. On the optical and thermal properties of in situ/ex situ reduced Ag NP's/PVA composites and its role as a simple SPR-based protein sensor. 2011; 1:87–96.
22. Samberg ME, Loboa EG, Oldenburg SJ, Monteiro-Riviere NA. Silver nanoparticles do not influence stem cell differentiation but cause minimal toxicity. 2012; 7:1197–1209.
23. Larese FF, D'Agostin F, Crosera M, Adami G, Renzi N, Bovenzi M, Maina G. Human skin penetration of silver nanoparticles through intact and damaged skin. Toxicology. 2009; 255:33–37. [PubMed: 18973786]
24. Samberg ME, Oldenburg SJ, Monteiro-Riviere NA. Evaluation of silver nanoparticle toxicity in skin in vivo and keratinocytes in vitro. 2010; 118:407–413.
25. Arora S, Jain J, Rajwade JM, Paknikar KM. Cellular responses induced by silver nanoparticles: In vitro studies. Toxicol Lett. 2008; 179:93–100. [PubMed: 18508209]
26. Trickler WJ, Lantz SM, Murdock RC, Schrand AM, Robinson BL, Newport GD, Schlager JJ, et al. Silver nanoparticle induced blood-brain barrier inflammation and increased permeability in primary rat brain microvessel endothelial cells. 2010; 118:160–170.
27. Ahamed M, Alsalhi MS, Siddiqui MK. Silver nanoparticle applications and human health. 2010; 411:1841–8.

28. Johnston HJ, Hutchison G, Christensen FM, Peters S, Hankin S, Stone V. A review of the in vivo and in vitro toxicity of silver and gold particulates: particle attributes and biological mechanisms responsible for the observed toxicity. 2010; 40:328–46.

29. Kumar R, Münstedt H. Silver ion release from antimicrobial polyamide/silver composites. Biomaterials. 2005; 26:2081–2088. [PubMed: 15576182]

30. Shi Q, Vitchuli N, Nowak J, Caldwell JM, Breidt F, Bourham M, Zhang X, et al. Durable antibacterial Ag/polyacrylonitrile (Ag/PAN) hybrid nanofibers prepared by atmospheric plasma treatment and electrospinning. 2011; 47:1402–1409.

31. Drake PL, Hazelwood KJ. Exposure-related health effects of silver and silver compounds: a review. Ann Occup Hyg. 2005; 49:575–585. [PubMed: 15964881]

32. Mukherjee SG, O'Claonadh N, Casey A, Chambers G. Comparative in vitro cytotoxicity study of silver nanoparticle on two mammalian cell lines. 2012; 26:238–251.

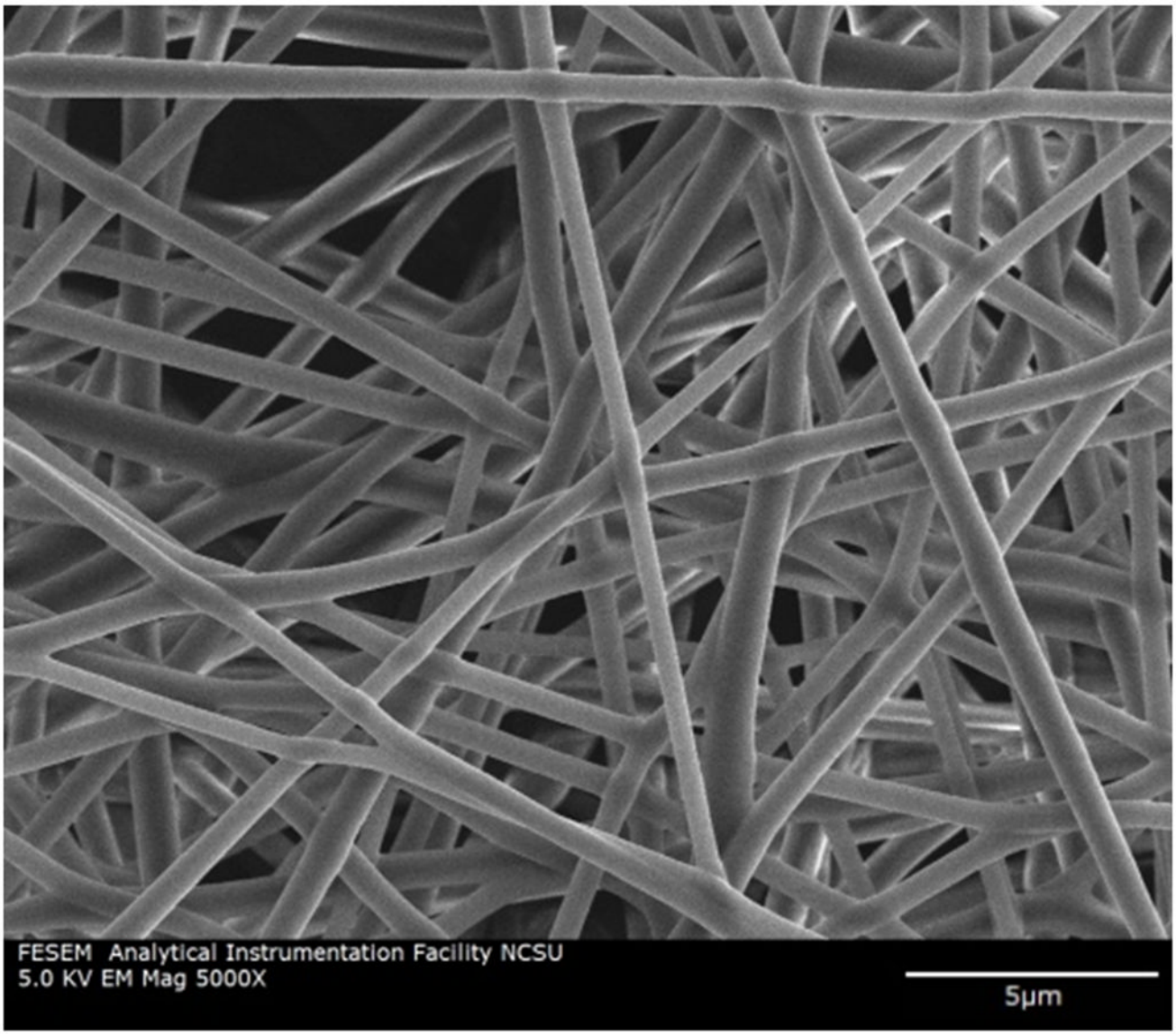

Figure 1.
SEM micrograph of PLA nanofibers

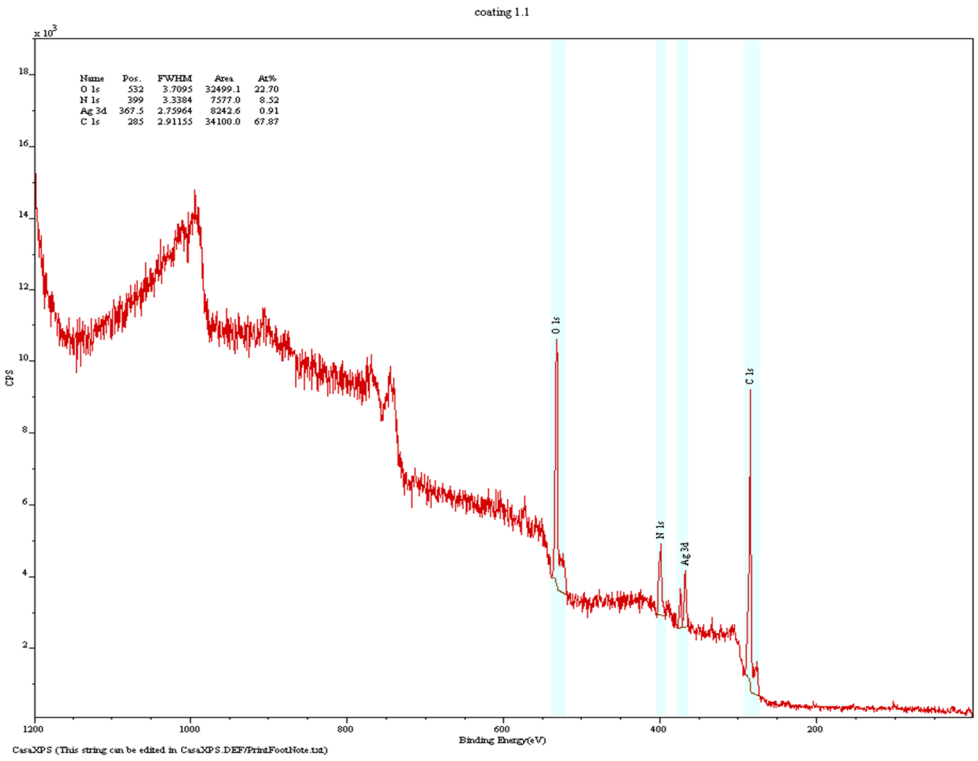

Figure 2.
XPS spectrum for PLA nanofibers coated with Silvadur ET (carbon and oxygen are components of PLA, nitrogen and silver are components of Silvadur ET).

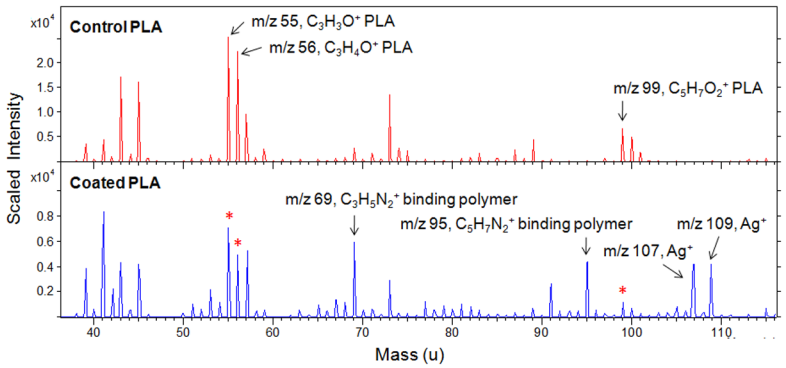

Figure 3.

TOF-SIMS spectra characterized by positive ion fragments for control and Silvadur ET (binding polymer + Ag) coated PLA nanofibers. Red stars on the coated PLA spectrum are assigned to the peaks related to control PLA, which are diminished after coating with Silvadur ET.

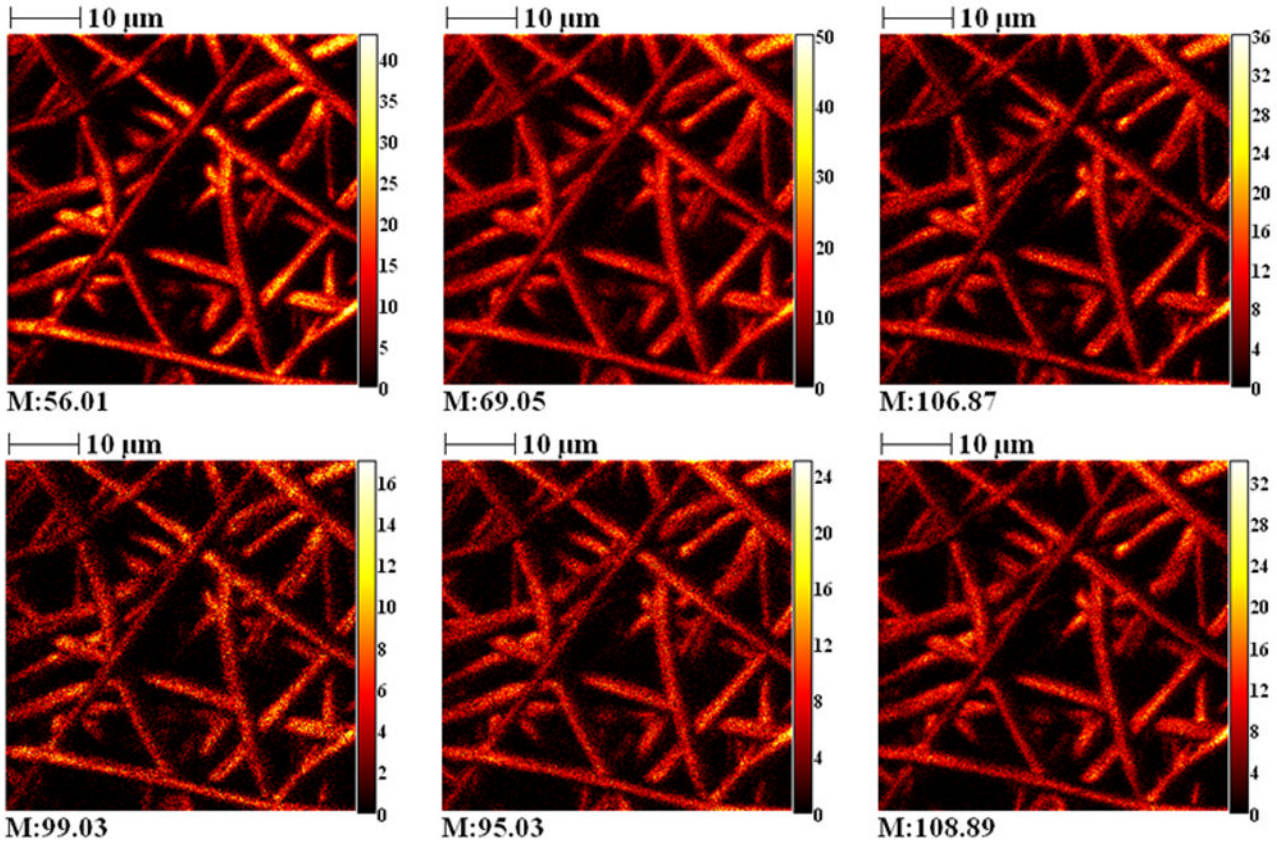

Figure 4.

TOF-SIMS chemical mapping of Silvadur ET coated PLA nanofibers indicating distribution and intensity of positive ions from PLA (M 56.01: $C_3H_4O^+$, M 99.03: $C_5H_7O_2^+$), binding polymer (M 69.05: $C_3H_5N_2^+$, M 95.03: $C_5H_7N_2^+$) and silver (M 106.87: Ag^+, M 108.89: Ag^+).

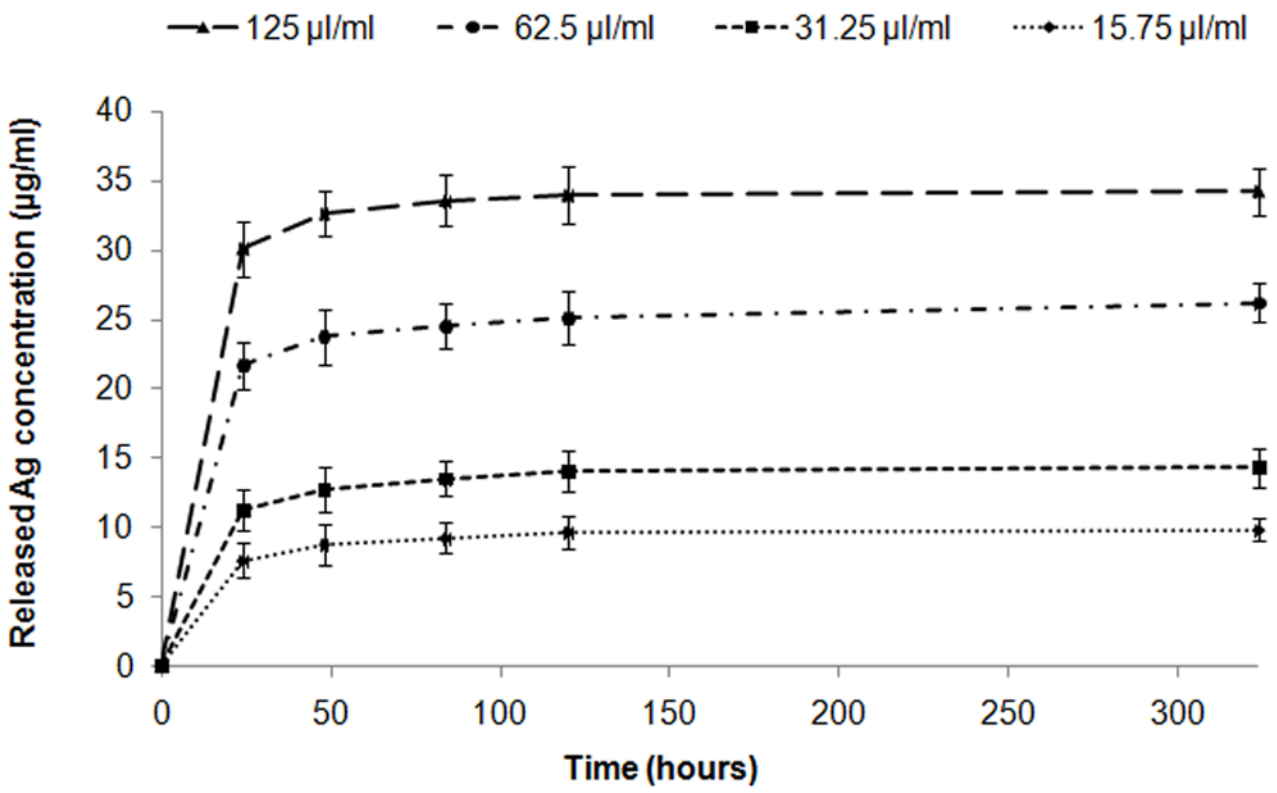

Figure 5.
Release profile of silver from PLA scaffolds coated with Silvadur ET containing different concentrations of silver varying from 15.75 μg/ml (bottom) to 125 μg/ml (top).

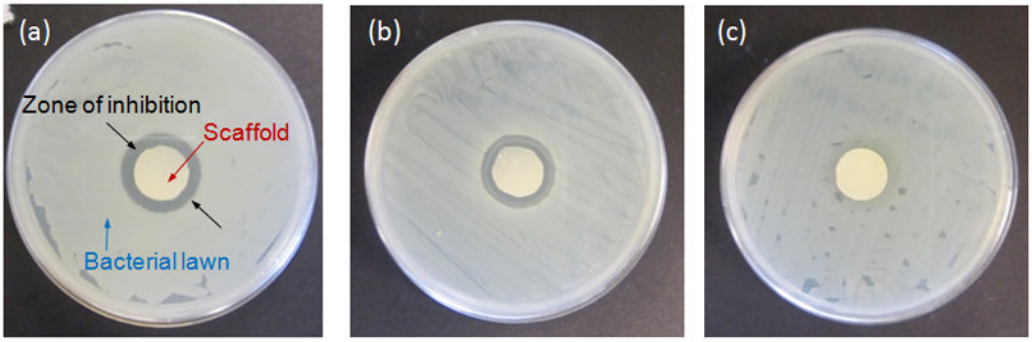

Figure 6.
Antimicrobial properties of scaffolds treated with Silvadur ET containing 31.25 μg/ml silver against *E. Coli* (a), *Staphylococcus aureus* (b), and silver resistant *E. Coli* (c) bacteria as evaluated via AATCC 147 test.

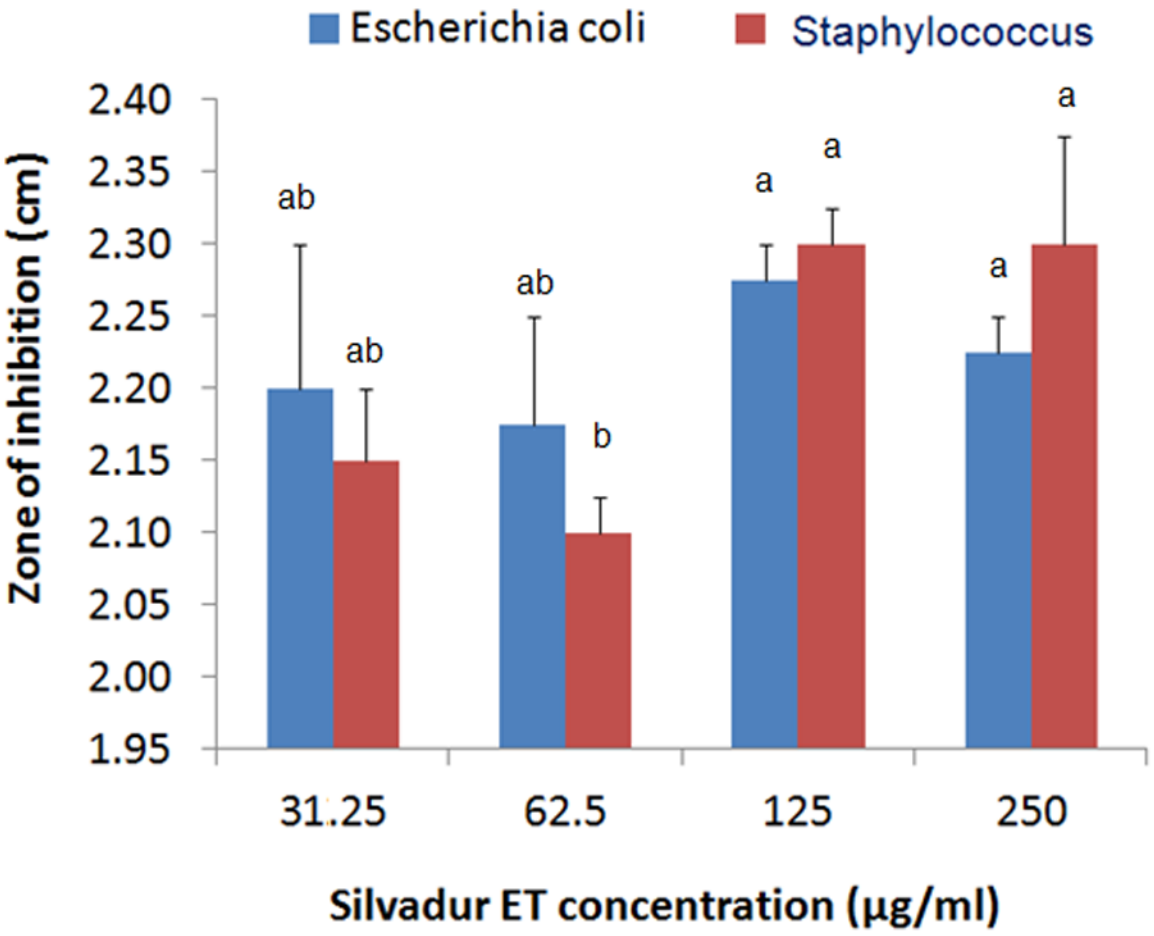

Figure 7.
Qualitative antimicrobial test (AATCC 147) for scaffolds coated with different concentrations of Silvadur ET. Columns with different letters indicate significant difference ($p<0.05$).

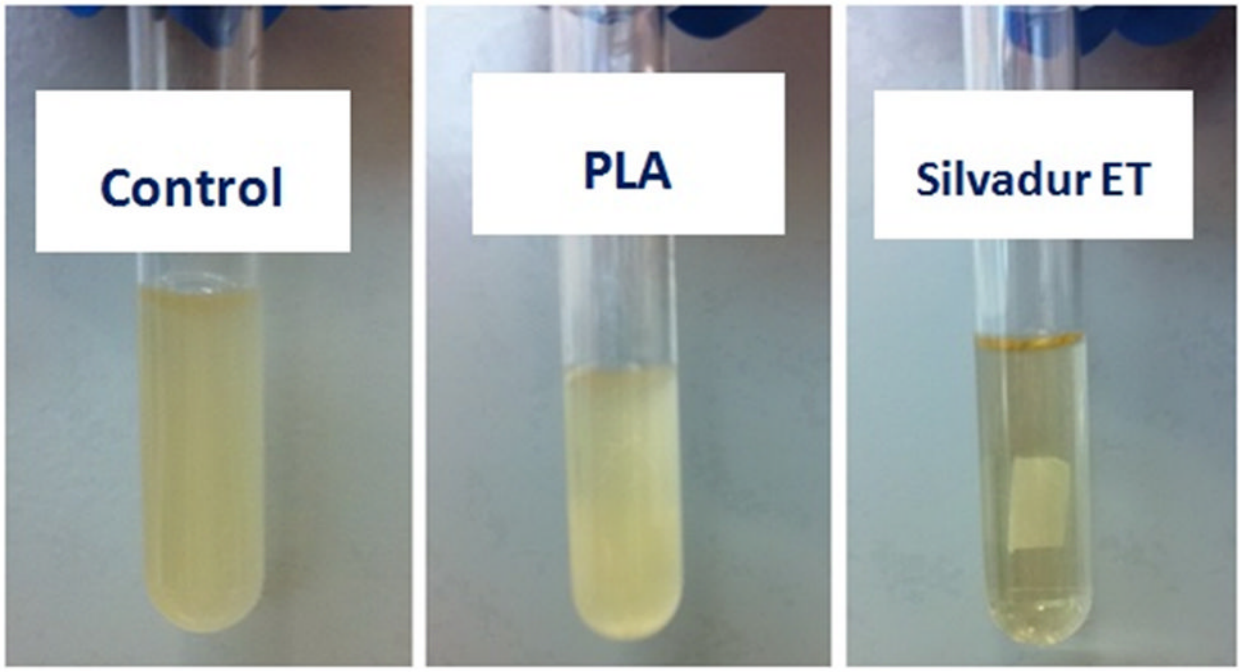

Figure 8.
Quantitative antimicrobial assessment (AATCC 100) of scaffolds coated with Silvadur ET containing 250 μg/ml silver in Silvadur ET coating solution. Cloudy color indicates bacterial contamination; clear color indicates lack of bacteria. 100% reduction was achieved for Silvadur ET coated scaffolds using equation (1).

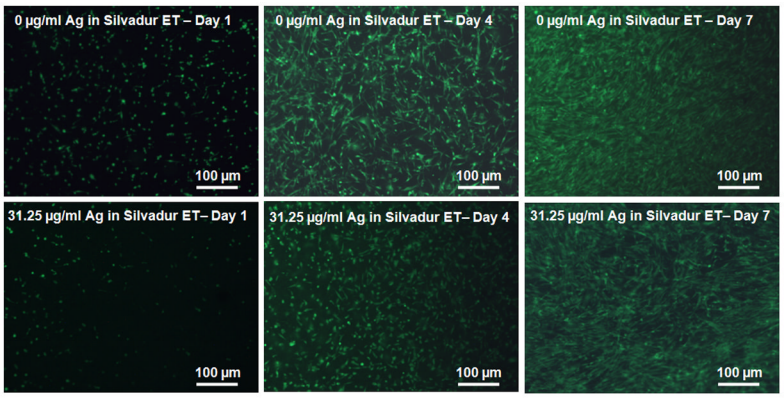

Figure 9.
Viability of human dermal fibroblasts on control (no silver, pure PLA alone) and antimicrobial (31.25 ug/mL silver in Silvadur ET coating of PLA fibers) scaffolds on days 1, 4 and 7.

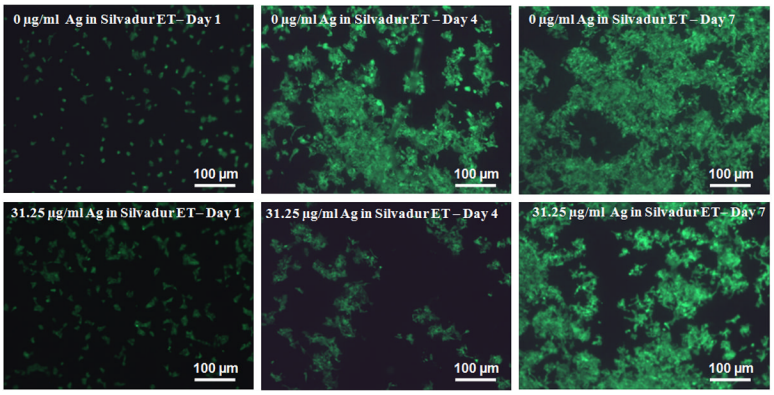

Figure 10.
Viability of human epidermal keratinocytes on control (no silver, pure PLA alone) and antimicrobial (31.25 ug/mL silver in Silvadur ET coating on PLA fibers) scaffolds on days 1, 4 and 7.

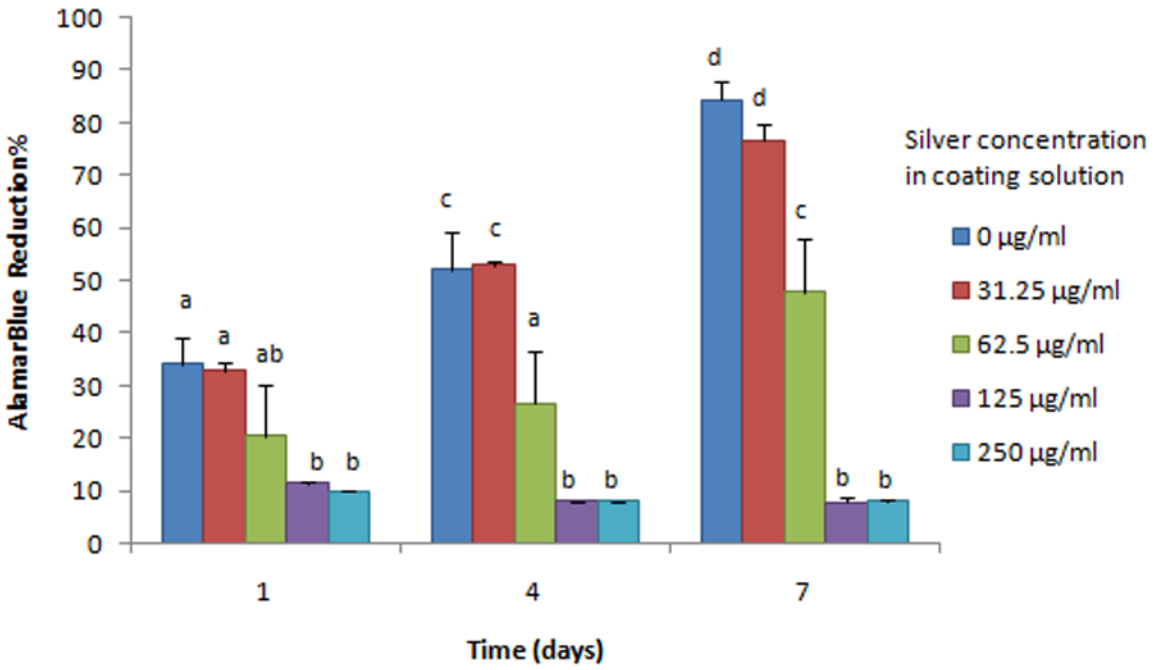

Figure 11.

AlamarBlue reduction for human dermal fibroblasts seeded on different scaffolds indicated that 31.25 ug/ml Silvadur ET concentration did not affect cell proliferation relative to 0 ug/ml control. Columns with different letters indicate significant difference ($p<0.05$).

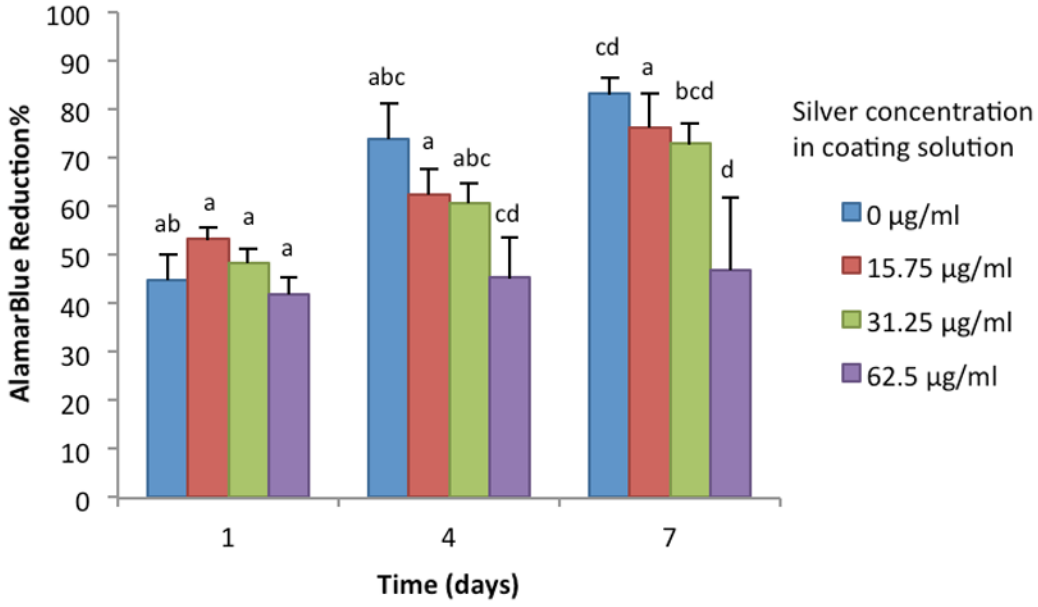

Figure 12.

AlamarBlue reduction for human epidermal keratinocytes seeded on scaffolds containing different silver concentrations indicated that 31.25 ug/ml Silvadur ET concentration did not affect cell proliferation relative to 0 ug/ml control. Columns with different letters indicate significant difference ($p<0.05$).

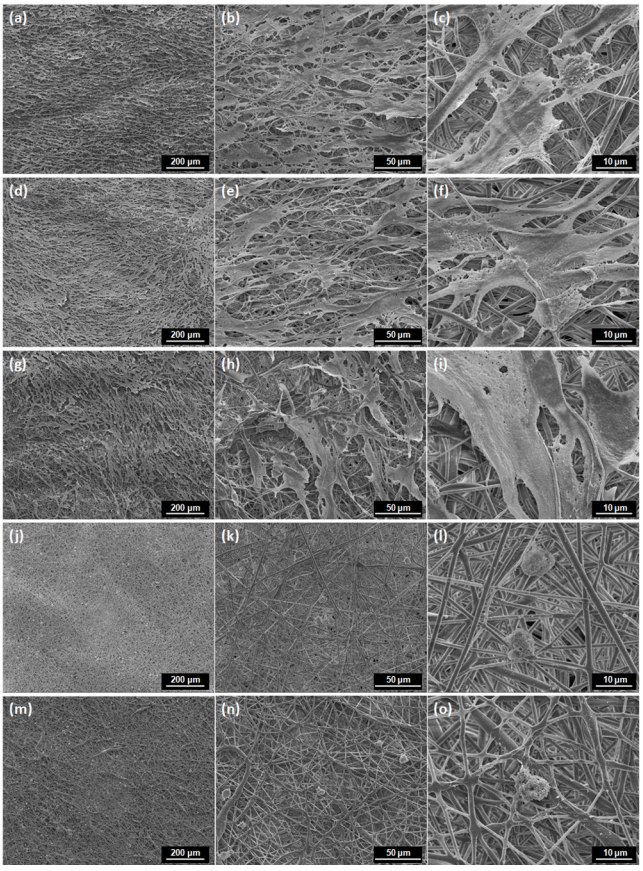

Figure 13.

SEM micrographs of human dermal fibroblasts seeded on pure PLA scaffolds (a, b, c), PLA antimicrobial scaffolds coated with Silvadur ET containing 31.25 μg/ml (d, e, f), 62.5 μg/ml (g,h, i), 125 μg/ml (j, k, l) and 250 μg/ml (m, n, p) silver at different magnifications of 100X, 500X, and 2000X (magnification increasing from left to right).

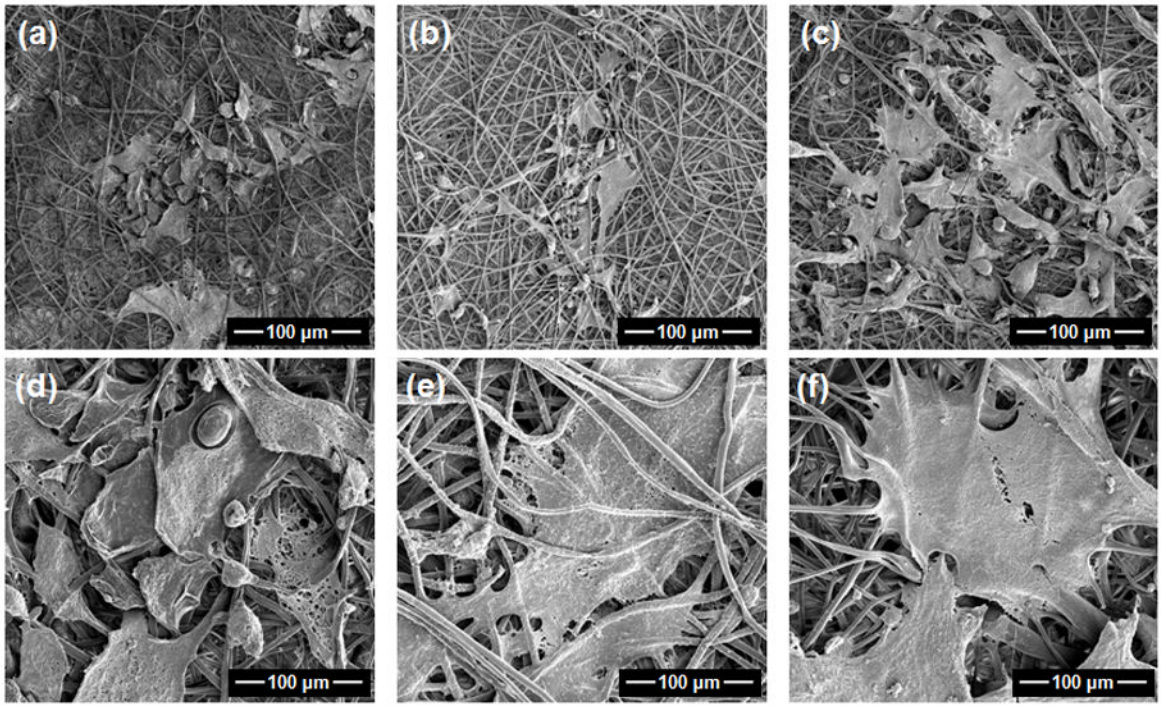

Figure 14.
SEM micrographs of human epidermal keratinocytes on antimicrobial scaffolds coated with Silvadur ET containing 15.75 μg/ml (a, c), 31.25 μg/ml (b, d), and 62.5 μg/ml (c, e) at different magnifications of 500X, and 2000X (magnifications increasing from top to bottom).